

Flow instabilities in polymer blends under shear

M. L. Fernandez*, J. S. Higgins and S. M. Richardson

Imperial College of Science, Technology and Medicine, Chemical Engineering

Department, Prince Consort Road, London SW7 2BY, UK

(Received 29 April 1994; revised 1 August 1994)

The effect of shear flow on the miscibility behaviour of the model polymer blend polystyrene/poly(vinyl methyl ether) has been investigated in real time by two-dimensional light scattering and optical microscopy. Under certain shear and dynamic temperature conditions large 'waves' have been observed which are aligned either in the direction parallel to the applied shear flow or just off it. Two-dimensional light scattering patterns from samples under the same conditions show sharp streaks aligned in the direction perpendicular to the flow. The evidence presented in this work indicates that these 'waves' are unlikely to be elongated phase-separated domains; instead, they could be caused by fluid instabilities.

(Keywords: polymer blends; shear flow; fluid instabilities)

INTRODUCTION

Flow fields have been observed to affect miscibility in both high and low molecular weight systems^{1,2}. While there has recently been a large number of experimental studies on polymer solutions under flow, data on polymer blends are still relatively scarce. One of the most popular techniques used to determine miscibility or phase separation is light scattering. This gives information on the shape and size of heterogeneities and can be used to follow the kinetics of phase separation. Light scattering is, therefore, a very useful technique for miscibility studies.

Several groups have recently published two-dimensional light scattering data on polymer mixtures under shear. Takebe *et al.*^{3–8} have studied the system polystyrene (PS)/polybutadiene in di-octyl phthalate sheared either in a Couette or in a cone-and-plate cell. From the scattering measurements the authors inferred the morphology of the sample being sheared. The measurements start in the quiescent state where the system is segregated macroscopically in two clear phases which lie one above the other in the shear cell. Under these conditions the system scatters very little light. When shear is applied to the system, a small-angle scattering signal is observed which the authors attributed to the interface breaking into droplets. As the shear rate is increased, the scattering pattern shows a streak elongated in the direction perpendicular to the shear flow. The authors argued that the streak arises from the droplets coalescing into large domains elongated in the direction parallel to the applied flow. At even higher shear rates the streak disappears and the level of scattering decreases dramatically. From these observations it was inferred that the sample becomes homogeneous at these shear rates. For this last regime (in which the system becomes homogeneous), the concentration fluctuations

are anisotropic, being strongly suppressed in the direction parallel to the shear flow.

Lyngaae-Jorgensen and Sondegaard^{9,10} have studied the styrene-acrylonitrile copolymer (SAN)/poly(methyl methacrylate) (PMMA) system in a cone-and-plate rheometer using two-dimensional light scattering. They started their measurements in the quiescent state by placing the system in the two-phase region of the phase diagram. Under these conditions the sample scatters light isotropically at small angles. When shear is applied the patterns become elongated in the direction perpendicular to the applied flow and at a critical shear rate the scattering disappears. The authors inferred that at this point the sample becomes homogeneous because, if the shear is then stopped, the isotropic scattering patterns return.

Werner *et al.*¹¹ investigated the system PS/(poly(vinyl methyl ether) (PVME) by two-dimensional light scattering and by excimer fluorescence. They carried out one measurement at a temperature at which the system in the quiescent state is homogeneous and then sheared the sample for 60 s at $\dot{\gamma} = 8 \text{ s}^{-1}$ in a parallel-plate cell. When shear is applied the scattering pattern first shrinks, then elongates and develops into a 'butterfly' pattern. The authors identified these findings with shear-induced phase separation. They also sheared a sample at $\dot{\gamma} = 16 \text{ s}^{-1}$ for 60 s at a temperature at which the system is phase separated in the quiescent state. With shear the scattering patterns elongate, then deform into a butterfly pattern and disappear. Finally the faint butterfly pattern returns and the authors argued that this is caused by oriented concentration fluctuations. At this point the sample is believed to be homogenized on the order of the wavelength of light.

Chen *et al.*^{12,13} have studied two systems: PS/polyisobutylene (PIB) and PS/PVME. The molecular weights for the former system were low and the mixture exhibits upper critical solution temperature (UCST) behaviour

* To whom correspondence should be addressed

while the latter shows lower critical solution temperature (LCST) behaviour like most high molecular weight polymer blends. The miscibility for the system PS/PIB was found to increase under shear. The system is placed in the two-phase region of the phase diagram under no shear. When shear is applied the scattering pattern becomes anisotropic and, as the shear rate is increased, the scattering eventually disappears. The authors inferred that the sample becomes homogeneous at this point. The behaviour of the system PS/PVME was investigated for two different molecular weights. For the case in which the molecular weights of the two components were low (but large enough that the system still shows LCST behaviour), the effects observed are similar to those reported for the system PS/PIB but the streak in the scattering pattern does not disappear either with time or shear rate. For the system PS/PVME (for PS of high molecular weight) distinctive scattering patterns were obtained. When shear is applied to the system in the two-phase region, the scattering pattern is H-shaped. With time, it develops into a dark streak perpendicular to the flow direction which does not disappear even after stopping the shear. Upon restarting the shear, the streak sharpens and develops into a bright streak.

Direct observation of the samples under shear flow is very uncommon. Besides our own work, to our knowledge only Kammer and co-workers¹⁴ have published any data. Kammer *et al.*¹⁴ studied the system SAN/PMMA in a parallel-plate cell. Microscopy was carried out at various radial positions and therefore shear rates. They observed spinodal decomposition in the centre of the sample where the shear rate is zero. At larger radial positions they observed elongated structures which they claimed are elongated phase-separated domains, arguing that this indicates shear-induced homogenization. Shear-induced mixing is also concluded from their turbidity measurements on the same system.

In this work we will present results from two-dimensional light scattering and from *in situ* optical microscopy for the blend PS/PVME as a function of temperature and shear rate. Some of our observations are similar to those reported by the above authors but we believe that our results could be explained by the existence of fluid instabilities rather than by arguments based on phase separation.

EXPERIMENTAL

Materials

The polymers used in this work were PS and PVME, supplied by Polymer Laboratories and by Scientific Polymer Products, respectively. Details on the characteristics of both polymers are indicated in Table 1. The appropriate amounts of each polymer were dissolved in toluene (18% w/v) and the resulting solutions were cast on glass plates under dry conditions. The films were kept under vacuum at approximately 30°C

until dry. The composition investigated was 30% by weight in PS, which is near the critical composition for the system.

Instrumentation

Rheometer. The shear cell used in these measurements has been described in detail elsewhere¹⁵. The sample is contained between two glass parallel plates. The bottom plate remains stationary while the top one rotates at a user-controlled speed between 0.095 and 4.54 rev min⁻¹. The whole assembly is placed inside a brass block which can be heated or cooled continuously, or maintained at a constant temperature. The bottom part of the cell stands on a freely rotating shaft with an extended arm resting on a calibrated spring. When shear is applied to the top plate, the lower part of the cell rotates as well. The displacement of the arm can be measured by means of a displacement transducer which gives values for the torque, and hence the viscosity and stress can be obtained. At the end of an observation the plate/sample/plate assembly can be quickly released and quenched for further measurements.

Two-dimensional light scattering. The light from an He/Ne 5 mW Aerotech laser impinged on a sample contained in the rheometer described above. The scattered light was imaged on a screen made from tracing paper and photographed with a Nikon camera (see Figure 1a).

In situ optical microscopy. The same rheometer as described above was used. The light source was a halogen lamp which was focused onto the sample with a Nikon condenser lens. The sample was then viewed by means of a charge-coupled device JVC video camera with a $\times 20$ lens. The image was recorded on a video tape (see Figure 1b).

Differential scanning calorimetry (d.s.c.). Some samples which had been observed directly by optical microscopy were released from the instrument and rapidly quenched in iced water followed by liquid nitrogen. The samples were not quenched directly in liquid nitrogen to prevent them from shattering due to the thermal shock. The samples were then viewed in a conventional optical microscope to make sure that the structure observed in the rheometer had been preserved by the quenching. The top plates were then removed and blend material was collected from the same positions at which the microscopy measurements had been taken. The quenched blends were measured by d.s.c. in a Perkin-Elmer instrument using a heating rate of 20°C min⁻¹ in all the runs.

RESULTS

In situ microscopy and two-dimensional light scattering

The cloud points for samples similar to the ones used in this work were measured in separate one-dimensional light scattering experiments. In the quiescent state the cloud point was approximately 129°C. For shear rates equal to 3 and 6 s⁻¹ the cloud point was approximately 133–134°C.

Samples were heated to 90, 100, 110, 115 and 120°C, either with no shear or at a shear rate of 3 or 6 s⁻¹. In

Table 1 Characteristics of the polymers used in this work

Polymer	M_w (g mol ⁻¹)	M_w/M_n	T_g (°C)	Refractive index, n
PS	96 000	1.04	107	1.59
PVME	95 000	2.5	-28	1.47

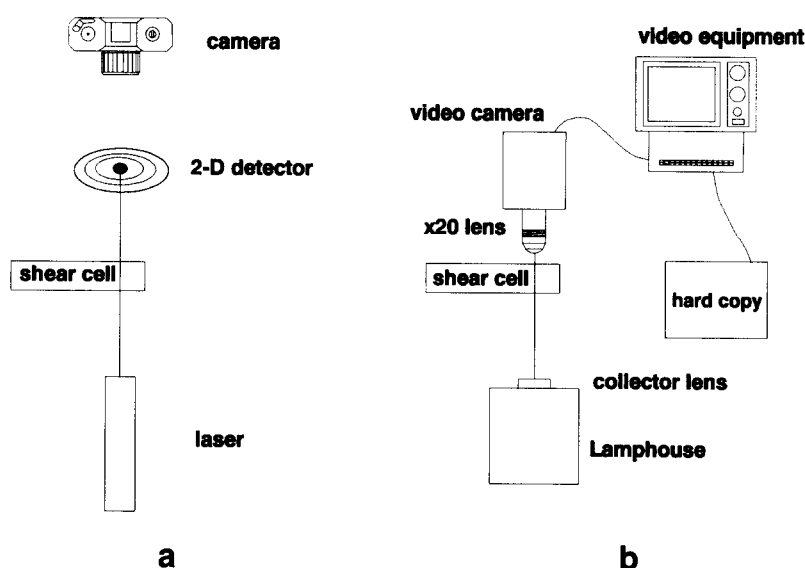


Figure 1 Schematic representations of the experimental set-up for (a) the two-dimensional light scattering measurements and (b) the *in situ* optical microscopy measurements

all cases the blend was clear and homogeneous and did not give rise to any scattering.

A sample was heated to 132°C under zero shear. At this temperature the sample was in the two-phase region of the phase diagram and showed a phase-separated structure on a submicron scale (see *Figure 2a*). The sample gave rise to a small-angle scattering signal which was isotropic (see *Figure 2b*). When a shear rate of 3 s^{-1} was applied, a large ($\sim 100 \mu\text{m} \times 5 \mu\text{m}$), dynamic, wave-like structure was observed superimposed on the submicron-sized phase separation (see *Figure 3a*). The appearance and evolution of these structures, which were recorded on video tape, are very informative. Since in this paper the structures are shown by taking snapshots of the video tape, we can only describe the dynamic aspect of the structures by analogies. The analogy that first springs to mind is that the structures observed and shown, for example, in *Figure 3* look like the waves on the surface of the sea when seen from a great height, such as from an aeroplane. The scattering pattern for a similar sample is shown in *Figure 3b*. The pattern shows an isotropic small-angle signal (which must arise from the phase-separated domains) superimposed on an intense streak which is oriented in the direction perpendicular to the flow and must be caused by the large 'waves' in the sample. As the sample was sheared continuously, it became transparent to the naked eye and the small-scale phase separation disappeared although the large waves persisted (see *Figure 4a*). It was difficult to determine accurately the time taken for the sample to become clear, but it was quite quick, of the order of 1 min or less. The scattering signal from a similar sample shows an intense streak perpendicular to the flow direction but no small-angle scattering (see *Figure 4b*). These findings are consistent with separate one-dimensional light scattering measurements which indicated that at this temperature and shear rates the effect of shear is to induce miscibility in the mixture.

Another sample was heated to 126°C under no shear. Under these conditions the sample was clear and homogeneous and did not scatter light. When shear was applied the sample was still clear to the naked eye but

under the microscope it showed waves similar to those in *Figure 4a*. The scattering pattern from a similar sample was analogous to that of *Figure 4b*, showing an intense streak in the direction perpendicular to the flow.

A final sample was heated to 136°C under no shear. Under these conditions the system is in the two-phase region of the phase diagram and the sample was phase-separated under the microscope. A similar sample showed a strong small-angle scattering signal which was isotropic. As has already been mentioned, from separate one-dimensional light scattering measurements it was determined that shear had no effect on the miscibility behaviour of the blend at this temperature for the shear rates used here. As the sample was sheared at 3 s^{-1} , the sample stayed cloudy and appeared phase-separated under the microscope. In addition, waves were observed although their size and intensity was somewhat smaller than those observed at 126 and 132°C. A similar sample showed a strong small-angle scattering signal superimposed on a streak oriented in the direction perpendicular to the flow. With time, the waves and the streak disappeared but the phase separation and the corresponding small-angle scattering persisted.

There are several reasons why it is unlikely that the waves seen in the light micrographs are elongated phase-separated domains as suggested by other authors. First, the appearance of the waves was distinctly different from phase separation, especially when seen in motion on the video tape. The waves were described above as resembling the surface of the sea seen from an aeroplane. On the video recording one could follow individual 'waves' forming, their 'crests' rising and falling and new waves forming. These observations are very different to the appearance of phase-separated domains.

Second, the waves are very long, of the order of $150 \mu\text{m} \times 5 \mu\text{m}$, and they appear in 5 or 6 s. If the waves were phase-separated domains, the diffusion coefficient required to cause the system to phase separate on such a large scale in such a short time would be unrealistically high. Taking the smallest dimension for the waves, $5 \mu\text{m}$, the diffusion coefficient necessary to give rise to a $5 \mu\text{m} \times 5 \mu\text{m}$ domain in 5 s would be $5 \times 10^{-8} \text{ cm}^2 \text{ s}^{-1}$.

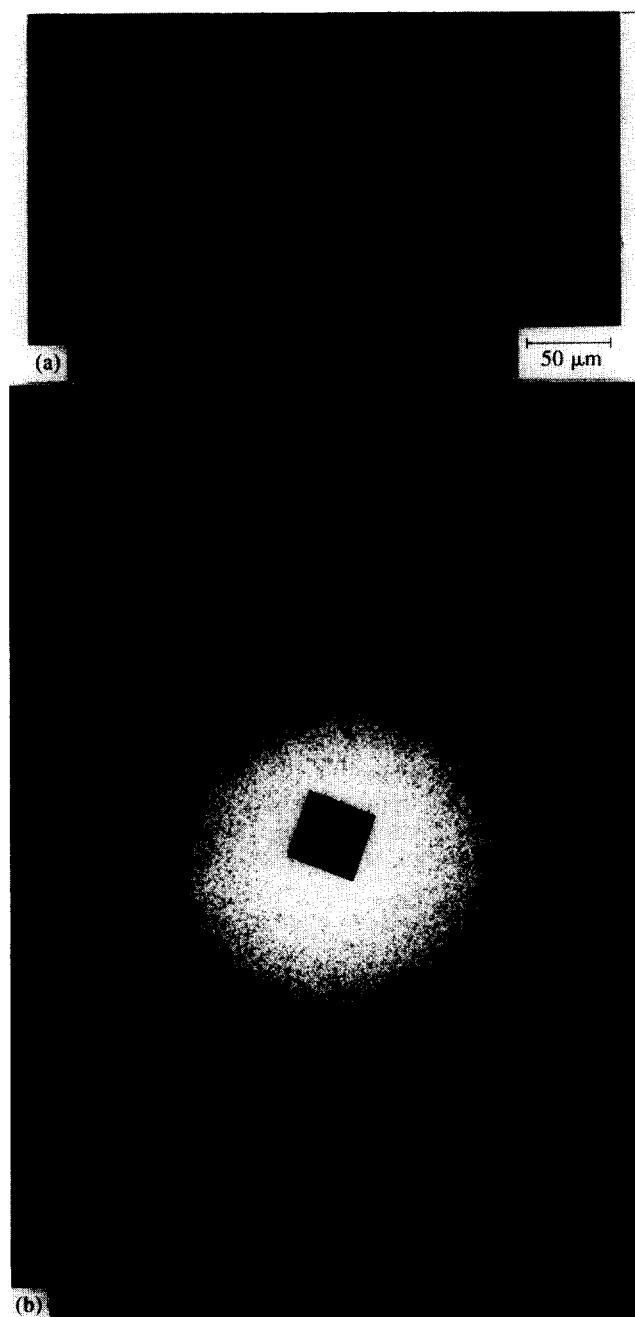


Figure 2 (a) Optical micrograph of a PS/PVME blend at 132°C in quiescent conditions. (b) Isotropic scattering signal obtained from a sample similar to that in (a). The position of the beam stop (black rectangle) is not exactly in the centre of the picture and this results in an apparent asymmetry in the photograph

Taking the overall wave size, $150\ \mu\text{m} \times 5\ \mu\text{m}$, the diffusion coefficient would have to be $1.5 \times 10^{-6}\ \text{cm}^2\ \text{s}^{-1}$ to give rise to such a large domain structure in 5 s. These values for the diffusion coefficient are approximately seven orders of magnitude larger than those found for the same system under quiescent conditions¹⁶, which are of the order of $10^{-13}\ \text{cm}^2\ \text{s}^{-1}$.

It is important to point out here that we have observed waves even in samples which have never been in the two-phase region of the phase diagram. Other authors only report results on measurements in which the sample

has been sheared from the two-phase region. If there were phase-separated domains already present in the sample, these could coalesce and form elongated domains under shear. In our case we have observed waves even at temperatures at which the sample was homogeneous in the quiescent state. Therefore, if our waves were elongated phase-separated domains they would have had to be

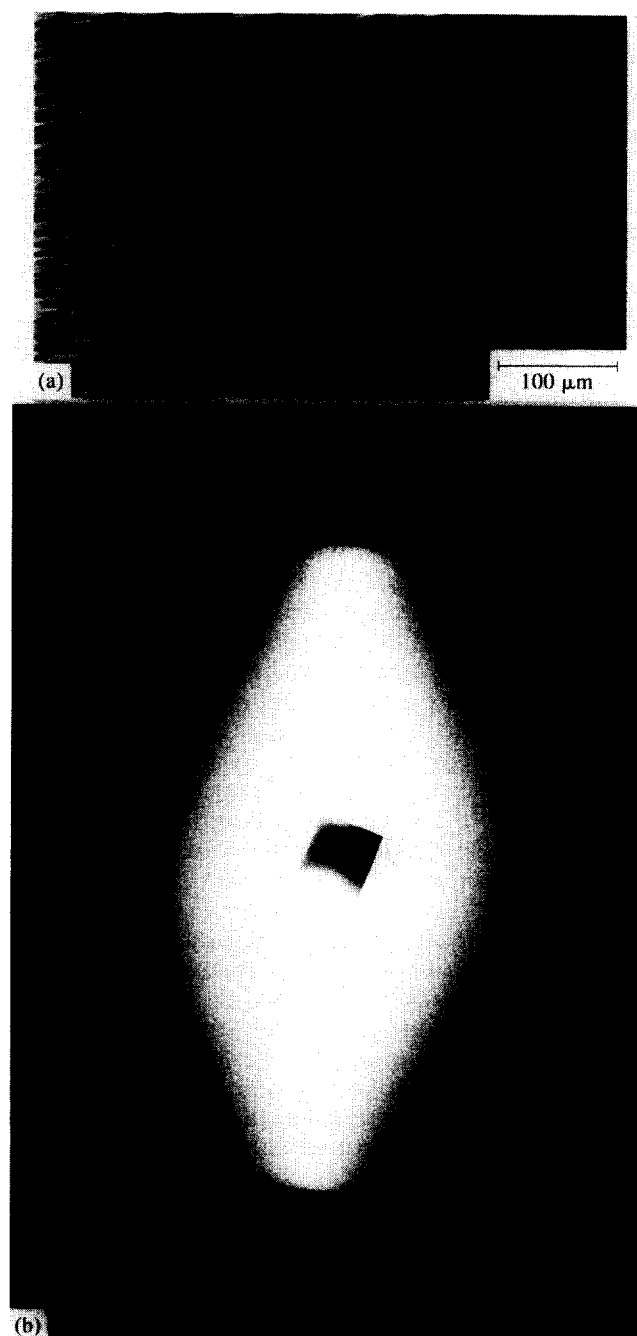


Figure 3 (a) Optical micrograph obtained for a sample of PS/PVME sheared at $T=132^\circ\text{C}$ and $\dot{\gamma} \approx 3\ \text{s}^{-1}$ for approximately 10 s. The direction of the shear was horizontal in the picture. Similar micrographs were obtained for samples sheared in the range $1\ \text{s}^{-1} \leq \dot{\gamma} \leq 16\ \text{s}^{-1}$ and $132^\circ\text{C} \leq T \leq 136^\circ\text{C}$. (b) Two-dimensional scattering pattern for a sample similar to that in (a). The sample was sheared at $\dot{\gamma} \approx 6\ \text{s}^{-1}$ and $T=132^\circ\text{C}$ for 10 s. The direction of the shear was horizontal in the picture. Similar results were obtained for other samples sheared in the range indicated in (a)

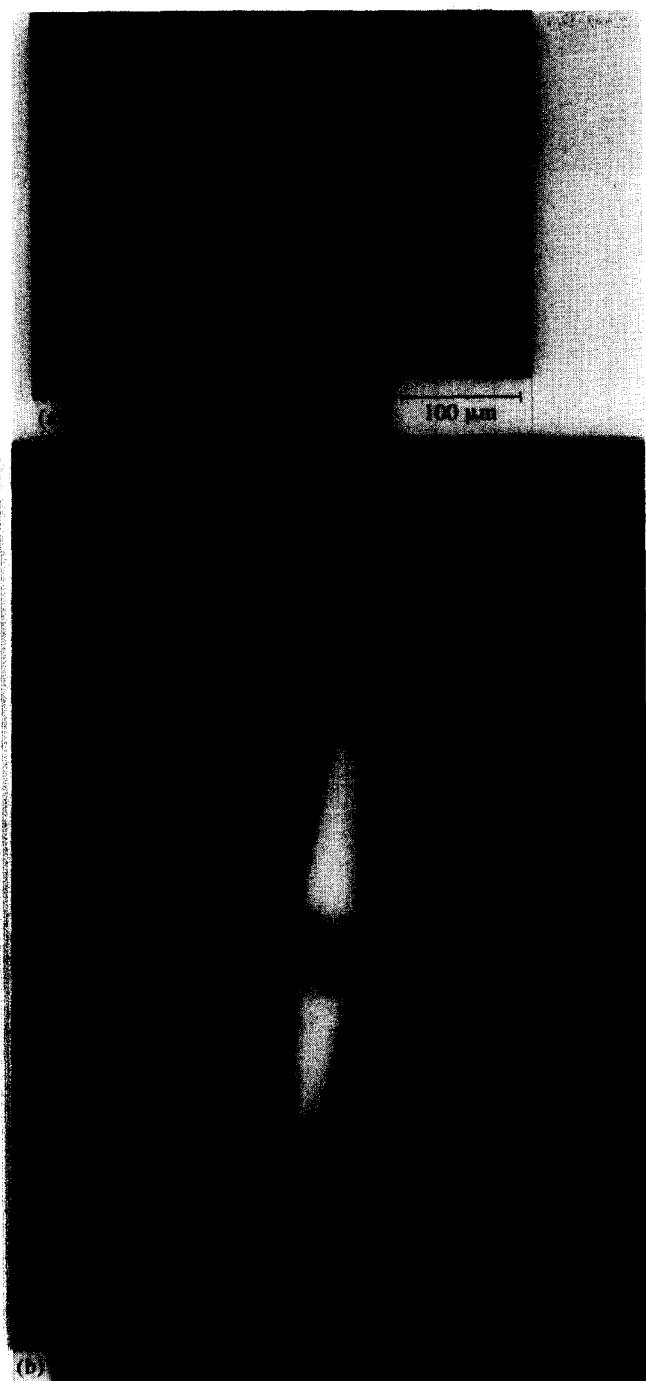


Figure 4 (a) Optical micrograph obtained for a sample of PS/PVME sheared at $T=132^{\circ}\text{C}$ and $\dot{\gamma}\approx 3\text{ s}^{-1}$ for approximately 10 min. The direction of the shear was horizontal in the picture. Similar micrographs were obtained for samples sheared in the range $1\text{ s}^{-1}\leq\dot{\gamma}\leq 16\text{ s}^{-1}$ and $126^{\circ}\text{C}\leq T\leq 129^{\circ}\text{C}$. (b) Two-dimensional scattering pattern for a sample similar to that in (a). The sample was sheared at $\dot{\gamma}=6\text{ s}^{-1}$ and $T=132^{\circ}\text{C}$ for 10 s. The direction of the shear was horizontal in the picture. Similar results were obtained for other samples sheared in the range indicated in (a)

formed by uphill diffusion and not by the coalescence of droplets that were already present.

Further information on the relaxation of the system which supports our contentions is described in the next section.

D.s.c. on quenched samples

A sample was heated at a shear rate of 1.5 s^{-1} to 128°C and equilibrated. The sample appeared clear to the naked

eye but under the microscope it showed waves as shown in Figure 5a. The sample was released rapidly from the instrument and quenched in iced water followed by liquid nitrogen. It was examined under a conventional phase contrast optical microscope to make sure that the structure observed in the rheometer had been preserved by the quenching procedure. This was clearly the case as shown in Figure 5b. The micrographs in Figures 5a and 5b are not identical because the magnification in the two instruments was different and also because the filters in the phase contrast microscope changed the colour of the micrographs. However, it is clear that the structure is similar in both micrographs and therefore the quenching procedure was effective. The top plate was removed and some blend material was scraped from the position at which the micrographs were taken. The resulting sample was analysed by d.s.c. and the thermograph showed a single glass transition at $T=-15.4^{\circ}\text{C}$ as shown in Figure 5c. The existence of a single glass transition at the same temperature as in unsheared 30/70 blend is consistent with the system being single phase.

A second sample was heated to 134.4°C at a shear rate of 2 s^{-1} and equilibrated. The sample appeared cloudy to the naked eye and under the microscope it showed waves superimposed on a smaller scale phase separation as shown in Figure 6a. The sample was quenched as for the previous case and the corresponding phase contrast optical micrograph is shown in Figure 6b. The two micrographs are not identical because of the different magnification and filter used, but the structure is clearly similar. The sample showed two glass transitions, one at $T_{g1}=-17.4^{\circ}\text{C}$ and a second at $T_{g2}=44.4^{\circ}\text{C}$, as shown in the bottom curve in Figure 6c. These two transitions are in between the transitions of the pure components and they appear at temperatures lower and higher, respectively, than that for the unsheared blend. The existence of two transitions together with their position are consistent with the sample being a two-phase system, with one of the phases being less than 30% in PS (that with $T_g=-17.4^{\circ}\text{C}$) and the second phase more than 30% in PS (that with $T_g=44.4^{\circ}\text{C}$). If the sample was then annealed in the d.s.c. pan for 30 min at 110°C , which is above the glass transition for the mixture but below the phase separation temperature, the sample remixed. This was confirmed by the presence of a single glass transition temperature at $T_g=-13.8^{\circ}\text{C}$ (see top curve in Figure 6c) which is very close to the T_g for the one-phase system in Figure 5 (the difference between -15.4 and -13.8°C is not significant).

From these results it is clear that the waves in the samples are not associated with a separate glass transition temperature and therefore it is unlikely that they are due to phase separation.

DISCUSSION

The effect of shear on the morphology and the scattering behaviour of the PS/PVME blend has been detailed in the previous section. Large wave-like structures have been observed under certain conditions of temperature and shear rate and they appear to be a phenomenon distinct from phase separation. Some further observations have been made which could throw light on the origin of the wave-like structures. Two-dimensional light scattering and *in situ* optical microscopy measurements were carried

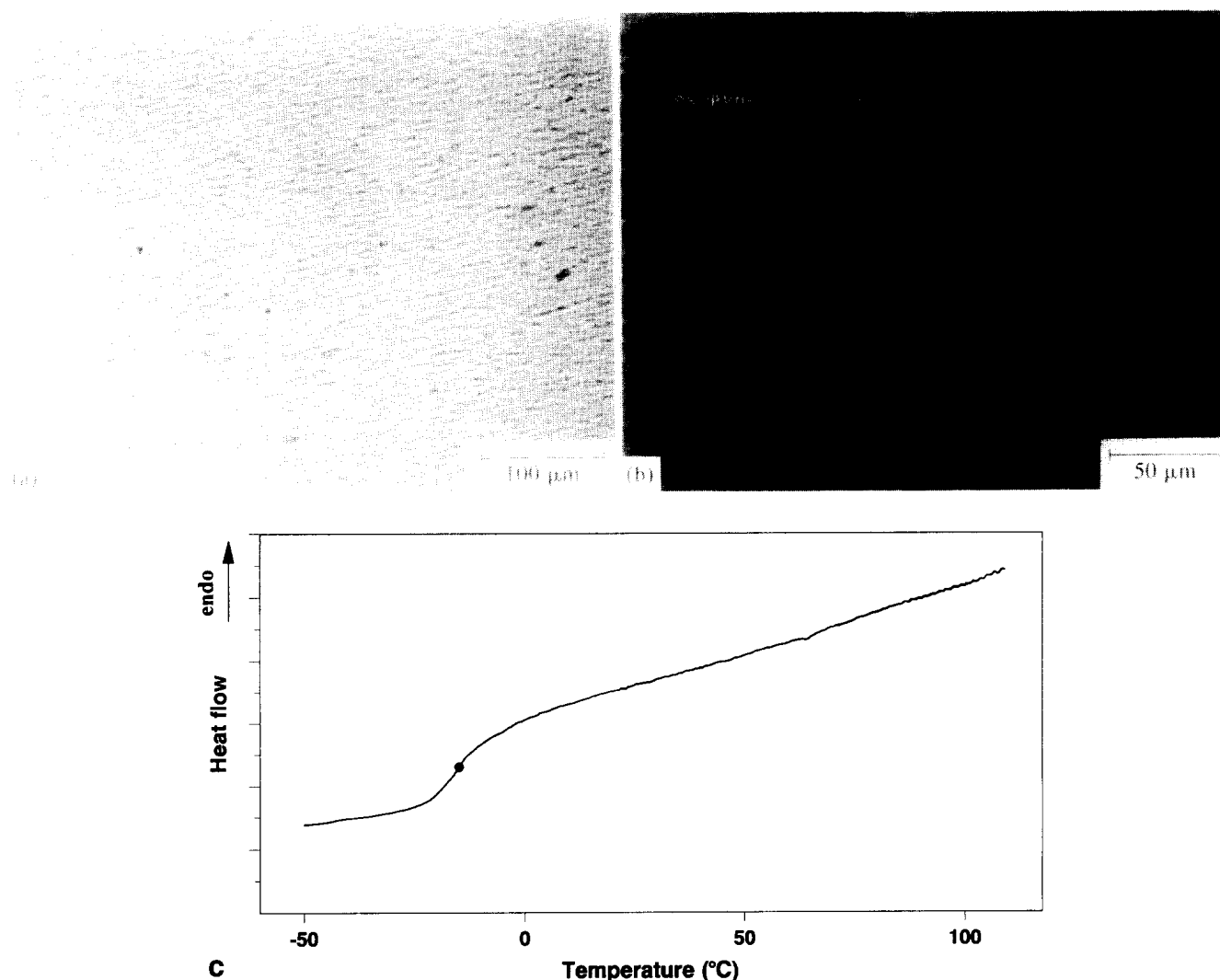


Figure 5 (a) Optical micrograph obtained for a sample of PS/PVME as it is being sheared at $T=128^{\circ}\text{C}$ and $\dot{\gamma}=1.5\text{ s}^{-1}$. The direction of the shear was horizontal in the picture. (b) Phase contrast optical micrograph obtained for the same sample after quenching in iced water followed by liquid nitrogen. The direction of the shear was horizontal in the picture. (c) D.s.c. trace for the previous sample, clearly showing one glass transition

out on a film of pure PVME and no waves or streaks were observed. In addition, for the blend the waves were observed to appear at temperatures near the phase boundary. These two facts suggest that the presence of the waves may be related in some way to the system being a blend, although the second observation could be totally coincidental. For the system ethyl vinyl acetate copolymer/solution chlorinated polyethylene no waves or streaks were detected. This system was much more viscous than the PS/PVME and it is possible that the presence or otherwise of the waves is related to the fluidity of the system.

One plausible explanation for the origin of the waves is that these are due to a fluid instability. It is well known^{17,18} that, for polymer mixtures in which there is a difference in the surface tension of the blend constituents, there could be a surface enrichment in the component with the lower surface energy. However, for the case of the PS/PVME blend, the PVME is known^{17,18} to segregate to the surface preferentially, even at room temperature. The films in our measurements were prepared by solvent casting and left to evaporate until dry. Therefore the samples would most likely have such an enriched surface layer before they were tested. If such

a layer existed, one could envisage a situation in which a fluid instability is set between the surface layer and the rest of the film. This would explain why pure PVME films do not show waves or streaks. Since the component with the lower surface tension segregates more readily the closer the system is to the phase boundary, this could explain why the waves are only observed at temperatures near the coexistence curves.

One phenomenon which could give rise to the waves observed is the Taylor–Saffman meniscus instability^{19–21}. This instability has been observed in liquids or very viscous adhesives. When voids or cracks propagate they show a transition from a stable smooth periphery to an unstable, finger-like one as the growth rate of the void increases. The same phenomenon is observed on grain boundaries in stressed solids. The original theory of Taylor and Saffman has been adapted and extended by Fields and Ashby²⁰ for the case of peeling situations, and they calculate expressions for the finger spacing and growth rate of the finger-like crack. For the fingers to grow, the pressure drop at the tips of the fingers must exceed the restraining effect of the surface tension, Γ , of the fluid. The larger the surface tension, the larger the finger spacing and therefore the more stable the interface.

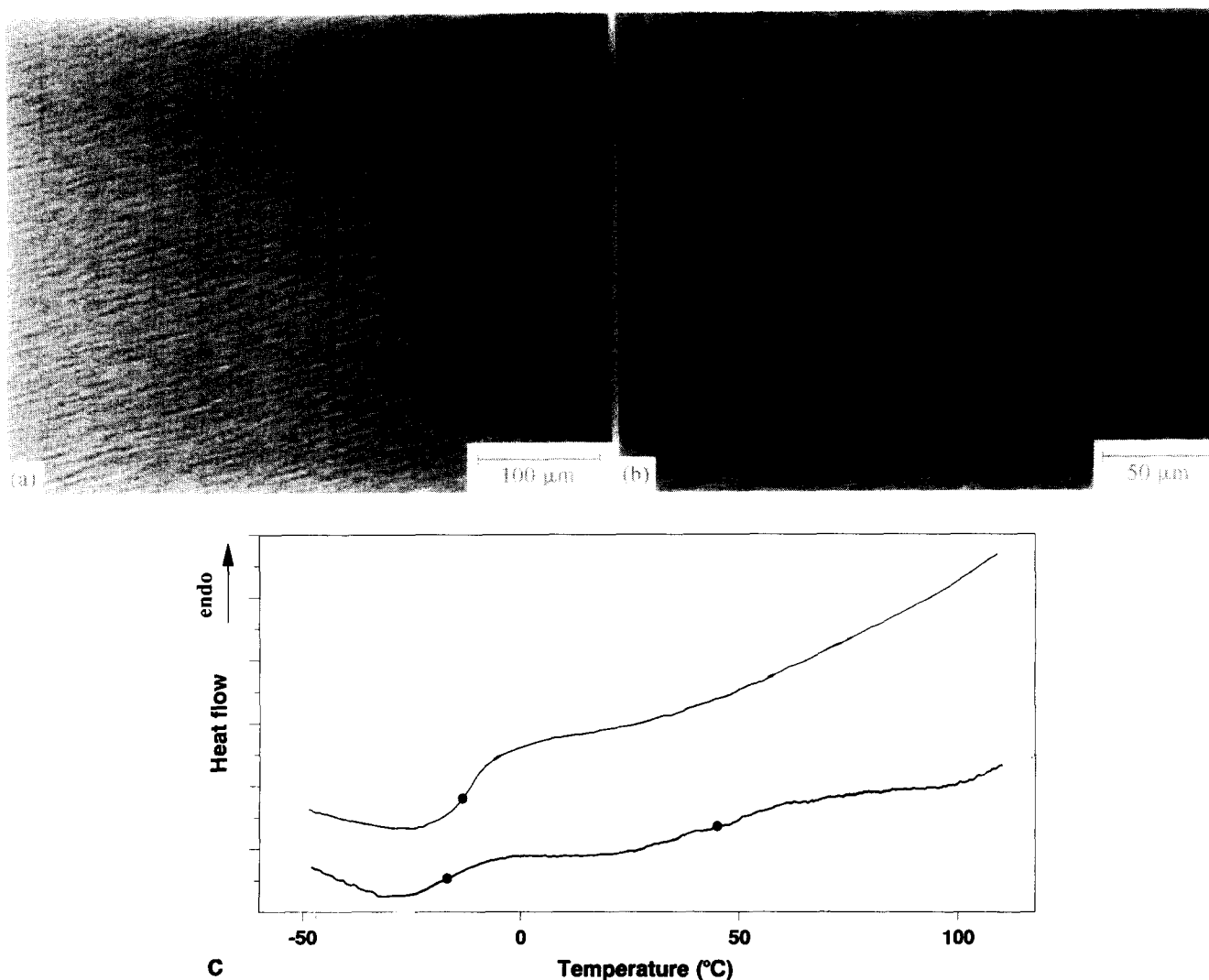


Figure 6 (a) Optical micrograph obtained for a sample of PS/PVME as it is being sheared at $T = 134.4^\circ\text{C}$ and $\dot{\gamma} = 2\text{ s}^{-1}$. The direction of the shear was horizontal in the picture. (b) Phase contrast optical micrograph obtained for the same sample after quenching in iced water followed by liquid nitrogen. The direction of the shear was horizontal in the picture. (c) D.s.c. traces for the previous sample as quenched (bottom curve) and after annealing at 110°C for 30 min (top curve). The sample as quenched shows clearly two glass transitions while the annealed sample shows a single glass transition

Fields and Ashby calculate the smallest finger spacing λ_{crit} that will grow and the steady-state finger spacing λ_{ss} for perfectly viscous (Newtonian) fluids, for perfectly plastic fluids and for viscoelastic materials:

$$\lambda_{\text{ss}} = \sqrt{\frac{\Gamma h^2}{6\alpha\eta v}} \quad (\text{Newtonian}) \quad (1)$$

$$\lambda_{\text{crit}} = \pi \sqrt{\frac{2\Gamma h}{\tau}} \quad (\text{plastic}) \quad (2)$$

where h is the film thickness, η is the fluid viscosity, τ is the shear stress, v is the peeling speed and α is a constant approximately equal to $1/4$. The difference between λ_{ss} and λ_{crit} is small and not important given the accuracy of the calculations. The expression for the viscoelastic fluids is more complicated and since we will only be carrying out approximate calculations, it is not necessary to include it here.

Values of viscosity for both pure PVME and for PS/PVME (30/70) were calculated by interpolation from the data of Green *et al.*²². The surface tension was calculated by interpolation from data of Bhatia *et al.*¹⁸

and v has been taken as the speed of the top plate. Since in our case it is not clear which value of thickness h should be used in equations (1) and (2) (i.e. the thickness of the enriched surface layer or the overall film thickness), the finger spacing λ was calculated as a function of h and temperature. The calculations indicate that, to obtain values of λ of the order of $10\text{ }\mu\text{m}$ as observed experimentally, the thickness of the film giving rise to the instability would have to be $\sim 10\text{--}30\text{ }\mu\text{m}$ (for 120 and 136°C respectively) for a perfectly plastic material and $\sim 50\text{--}100\text{ }\mu\text{m}$ (for 120 and 136°C respectively). These thicknesses are larger than the hypothetical surface-enriched layer but smaller than the overall film thickness. Given the number of assumptions made in these calculations we can conclude that the order of magnitude that we obtain for h is reasonable and the Taylor–Saffman instability could explain the phenomena observed in our films.

The calculations also show that for a constant value of h , λ increases with temperature. From our *in situ* optical micrographs it is difficult to measure any change in the finger spacing accurately. However, it is clear that as the temperature is increased the waves become progressively less evident. This is consistent with the results of the

calculations, which predict a suppression of the instability for high temperatures.

From the calculations carried out at 110°C, the instability should not be suppressed at this temperature. The fact that the instability is not observed at this temperature could indicate that only measurements carried out near the phase boundary, where surface enrichment is accelerated, give rise to a sufficiently large surface film and hence to an instability.

Calculations for a film of pure PVME show that given the values of viscosity, surface tension, thickness and shear rate, fingering due to the Taylor–Saffman instability should be observed. The fact that no instability was observed for this film in the wide range of temperatures explored (50 to 130°C) could indicate that the second fluid layer is necessary for giving rise to the fingers or waves observed for the PS/PVME blend. Alternatively, there could be an instability in the film but the absence of separate layers might make it impossible to detect.

The existence or otherwise of a surface layer enriched in PVME could be proved by analysing and comparing the compositions of the surface and the bulk. Unfortunately, the films tend to break up during the quenching and therefore these measurements have been impossible to perform to date.

In summary, the calculations carried out assuming that the cause of the waves is the Taylor–Saffman instability give reasonable values for the film thickness h . This does not mean that this is the actual instability taking place. Another possibility, for example, is the Kelvin–Helmholtz instability¹⁹.

The Kelvin–Helmholtz instability arises at the interface between two superposed fluids which flow one over the other with a relative horizontal velocity. For two uniform fluids, an upper fluid of density ρ_2 and a lower fluid of density ρ_1 with constant velocities U_2 and U_1 , respectively, the Kelvin–Helmholtz instability will be suppressed if

$$(U_1 - U_2)^2 < \frac{2}{\alpha_1 \alpha_2} \sqrt{\frac{\Gamma g(\alpha_1 - \alpha_2)}{\rho_1 + \rho_2}} \quad (3)$$

where Γ is the surface tension, g is the acceleration due to gravity ($=9.81 \text{ m s}^{-2}$), $\alpha_1 = \rho_1/(\rho_1 + \rho_2)$ and $\alpha_2 = \rho_2/(\rho_1 + \rho_2)$. The wavelength of the waves l formed by the instability is given by

$$l = \frac{2\pi\alpha_1\alpha_2(U_1 - U_2)^2}{2g(\alpha_1 - \alpha_2)} \quad (4)$$

and the wave velocity v by

$$v = \alpha_2|U_1 - U_2| \quad (5)$$

Values for the densities of pure PVME and the PS/PVME blend at room temperature were obtained from Yang *et al.*²³: $\rho_{\text{PVME}} = 1.047 \text{ g cm}^{-3}$ and $\rho_{\text{blend}} = 1.058 \text{ g cm}^{-3}$. The dependence of PVME density on temperature was obtained from the data of Uriarte *et al.*²⁴:

$$\rho_{\text{PVME}}(t) = \rho_{\text{PVME}}(25^\circ\text{C}) - 7.388 \times 10^{-4}(t - 25) - 2.867 \times 10^{-7}(t - 25)^2$$

and the same relationship was used for the dependence of the blend density with temperature. In the following calculations we have assumed that the PVME segregates preferentially to the surface of the samples and that our

films are therefore stratified with pure PVME on the top and PS/PVME at the bottom. For the temperature range between 110 and 136°C, the results show that values of $(U_1 - U_2) \leq 0.20\text{--}0.26 \text{ cm s}^{-1}$ will suppress the instability. These speeds are of the same order as the speed of the top rotating plate in the set-up used in the present work ($0.23\text{--}0.33 \text{ cm s}^{-1}$). Therefore, if this treatment were correct and the waves observed by *in situ* microscopy are due to the Kelvin–Helmholtz instability, our samples would have to show an almost immobile bottom layer of PS/PVME and a top layer of PVME which rotates at the same speed as the top glass plate in our set-up. However, given the approximations made in these calculations, one should not attach much importance to the actual values obtained. From equations (4) and (5), the values for the wavelength and velocity of the waves are approximately $90\text{--}150 \mu\text{m}$ and $0.10\text{--}0.13 \text{ cm s}^{-1}$, respectively, depending on the temperature, which agree well with our rheo-microscopy observations.

In summary, it is possible that the relative motion of a top layer enriched in PVME and a bottom layer of PS/PVME gives rise to a Kelvin–Helmholtz instability and the values obtained for the wavelength and velocity of the waves compare well with the values obtained by *in situ* microscopy.

As detailed in the Introduction, other authors have observed highly elongated scattering patterns similar to the ones presented here. The majority of these experiments have been carried out by applying shear to a system which is in the two-phase region. Under these conditions the droplets present in the system in the quiescent state could coalesce and form very elongated phase-separated domains which would then give rise to a streak in the scattering patterns. At this point, we cannot discuss whether the streaks observed by these authors arise from a similar phenomenon to the one we have observed. However, the possibility that fluid instabilities could give rise to streaks in the scattering patterns should be considered, especially given the relatively fluid nature of most of the systems investigated.

CONCLUSIONS

The effect of shear flow on morphology and miscibility has been investigated for the model polymer blend PS/PVME. The techniques used were two-dimensional light scattering and *in situ* optical microscopy. Under certain conditions of temperature and shear rate, large waves oriented in the direction of the flow were observed by microscopy. These gave rise to an intense streak in the two-dimensional scattering patterns, elongated in the direction perpendicular to the flow. It is unlikely that these waves are due to phase separation as proposed by other authors for other systems and experimental conditions. Instead, they could be due to a fluid instability between a PVME-enriched surface layer and the rest of the film. The Taylor–Saffman meniscus instability is a possible explanation for these observations, and calculations for the finger spacing give the correct order of magnitude for the film thickness. Another plausible explanation for our observations is the Kelvin–Helmholtz instability, and the experimental values obtained for the wavelength and velocity of the waves agree well with the theoretical predictions. Although in this work we have considered only two types of instabilities that could be

present in the system, these are clearly not the only possibilities. The purpose of this paper is to point out that fluid instabilities must be considered when carrying out rheo-scattering or rheo-microscopy measurements and not to establish which instability is present in our particular case. Clearly, more experiments would be required to determine that point.

ACKNOWLEDGEMENTS

The authors would like to thank Professors B. A. Wolf, R. J. Young and W. A. Weiss for their helpful ideas and suggestions, Mr C. Haddow for taking the scattering pictures and the SERC for financial support.

REFERENCES

- 1 Rangel-Nafaile, C., Metzner, A. and Wissburn, K. *Macromolecules* 1984, **17**, 1187
- 2 Hindawi, I. A. *PhD thesis*, Imperial College, London, 1991
- 3 Takebe, T., Sawaoka, R. and Hashimoto, T. *J. Chem. Phys.* 1989, **91**, 4369
- 4 Takebe, T. and Hashimoto, T. *Polym. Commun.* 1988, **29**, 227
- 5 Takebe, T. and Hashimoto, T. *Polym. Commun.* 1988, **29**, 261
- 6 Takebe, T., Hashimoto, T. and Fujioka, K. 'Proc. 4th Nishinomiya-Yukawa Symp. on Theoretical Physics', Nishinomiya City, Japan, 1989
- 7 Hashimoto, T., Takebe, T. and Suehiro, S. *J. Chem. Phys.* 1988, **88**, 5874
- 8 Takebe, T., Fujioka, K., Sawaoka, R. and Hashimoto, T. *J. Chem. Phys.* 1990, **93**, 5271
- 9 Lyngaae-Jorgensen, J. and Sondegaard, K. *Polym. Eng. Sci.* 1987, **27**, 351
- 10 Sondegaard, K. and Lyngaae-Jorgensen, J. 'Polymer Rheology and Processing' (Eds A. A. Collyer and L. A. Utracki), Elsevier Applied Science, New York, 1990
- 11 Werner, D. E., Fuller, G. G. and Frank, C. W. 'Proc. XIth Int. Congr. on Rheology', Belgium, 1992
- 12 Chen, Z. J., Shaw, M. T. and Weiss, R. A. *Proc. ACS PMSE Div.* 1994, **71**, 123
- 13 Chen, Z. J., Wu, R.-J., Shaw, M. T., Weiss, R. A., Fernandez, M. L. and Higgins, J. S. *Polym. Eng. Sci.* in press
- 14 Kammer, H. W., Kummerloewe, C., Kressler, J. and Melior, J. P. *Polymer* 1991, **32**, 1488
- 15 Hindawi, I. A., Higgins, J. S. and Weiss, R. A. *Polymer* 1992, **33**, 2522
- 16 Hashimoto, T. in 'Current Topics in Polymer Science' (Eds Ottenbrite, Utracki and Inoue), Vol. II, Hanser Verlag, Munich, 1987, Ch. 6.1, p. 230
- 17 Pan, D. H. and Prest, W. M. *J. Appl. Phys.* 1985, **58**, 2861
- 18 Bhatia, Q. S., Pan, D. H. and Koberstein, J. T. *Macromolecules* 1988, **21**, 2166
- 19 Chandrasekar, S. 'Hydrodynamic and Hydromagnetic Instability', Clarendon Press, Oxford, 1961
- 20 Fields, R. J. and Ashby, M. F. *Phil. Mag.* 1976, **33**, 33
- 21 O'Kane, W. J. and Young, R. J. *J. Adhes.* 1993, **41**, 203
- 22 Green, P. F., Adolf, D. B. and Gilliom, L. R. *Macromolecules* 1991, **24**, 3377
- 23 Yang, H., Shibayama, M., Stein, R. S., Shimizu, N. and Hashimoto, T. *Macromolecules* 1986, **19**, 1667
- 24 Uriarte, C., Iruin, J. J., Fernandez-Berridi, M. J. and Elorza, J. M. *Polymer* 1989, **30**, 1155